

UC Irvine

UC Irvine Previously Published Works

Title

The two-phase flow downstream of a production engine combustor swirl cup

Permalink

<https://escholarship.org/uc/item/3vx6q1nv>

Journal

Symposium (International) on Combustion, 24(1)

ISSN

0082-0784

Authors

Wang, HY
McDonell, VG
Samuelsen, GS

Publication Date

1992

DOI

10.1016/s0082-0784(06)80170-0

Copyright Information

This work is made available under the terms of a Creative Commons Attribution License, available at <https://creativecommons.org/licenses/by/4.0/>

Peer reviewed

Scaling of the Two-Phase Flow Downstream of a Gas Turbine Combustor Swirl Cup: Part I— Mean Quantities

H. Y. Wang

V. G. McDonell

W. A. Sowa

G. S. Samuelsen

UCI Combustion Laboratory,
University of California,
Irvine, CA 92717-3550

A production gas turbine combustor swirl cup and a 3×-scale model (both featuring co-axial, counterswirling air streams) are characterized at atmospheric pressure. Such a study provides an opportunity to assess the effect of scale on the behavior of the continuous phase (gas in the presence of spray) and droplets by comparing the continuous phase velocity, droplet size, and droplet velocity at geometrically analogous positions. Spatially resolved velocity measurements of the continuous phase, droplet size, and droplet velocity were acquired downstream of the production and 3×-scale swirl cups by using two-component phase-Doppler interferometry in the absence of reaction. While the continuous phase flow fields scale well at the exit of the swirl cup, the similarity deviates at downstream locations due to (1) differences in entrainment, and (2) a flow asymmetry in the case of the production hardware. The droplet velocities scale reasonably well with notable exceptions. More significant differences are noted in droplet size, although the presence of the swirl cup assemblies substantially reduces the differences in size that are otherwise produced by the two atomizers when operated independent of the swirl cup.

Introduction

Co-axial, counterswirling air streams have been studied for a variety of applications in combustion and other systems. Most of the studies have been conducted at nonreacting, single-phase (i.e., gas phase in the absence of spray) conditions. Some of these studies (e.g., Habib and Whitelaw, 1980; Vu and Gouldin, 1982; Gouldin et al., 1983) observe that only counterswirl produces recirculation, while others (e.g., Samimy and Langenfeld, 1988; Mehta et al., 1989) find that both coswirl and counterswirl can generate a recirculation zone.

One of the practical applications featuring two co-axial counterswirling streams is the GE SNECMA CFM56 engine combustor swirl cup (Fig. 1). Fuel is injected by a simplex atomizer mounted in the center of the swirl cup. A portion of the droplets convect directly downstream while the remainder impinge onto the inner surface of a primary venturi (which separates the primary swirling air from the secondary swirling air), form a thin liquid film, and are re-atomized in the shear field produced between the two counterswirling air streams. A goal of this swirl cup assembly is to produce a uniformly distributed field of similarly sized fine droplets.

Contributed by the International Gas Turbine Institute and presented at the 37th International Gas Turbine and Aeroengine Congress and Exposition, Cologne, Germany, June 1-4, 1992. Manuscript received by the International Gas Turbine Institute February 6, 1992. Paper No. 92-GT-207. Associate Technical Editor: L. S. Langston.

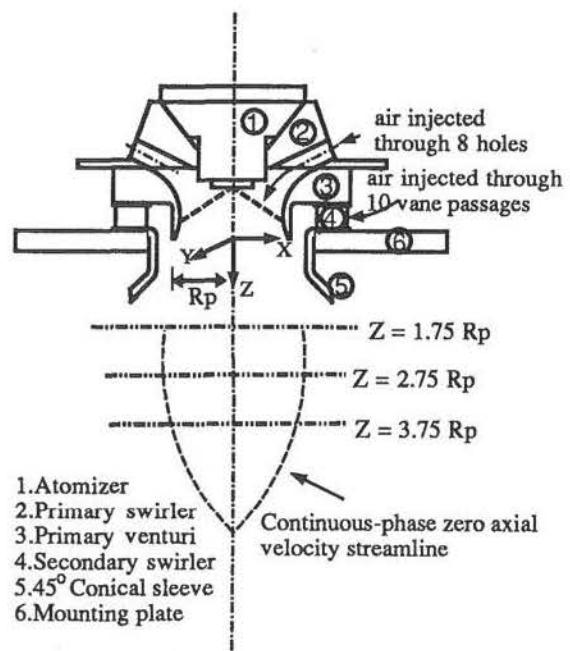


Fig. 1 Swirl cup assembly

Table 1 Characteristics of the PDI

	1 ×	3 ×
Transmitter		
0.5145 μm line (<i>U</i> , <i>D</i>)*		
Fringe spacing (μm)	9.03	9.88
Waist (μm)	223.32	187.17
0.4880 μm line (<i>V</i> or <i>W</i>) ²		
Fringe spacing (μm)	9.31	9.84
Waist (μm)	211.82	177.53
Receiver		
Collection lens (mm)	629 f/5.7	1000 f/9.3
Focusing lens (mm)	238	238
Spatial filter (μm)	100	100
Collection angle	30 deg off-axis forward	

**U*, *V*, *W*, and *D* are axial, radial, tangential velocity, and droplet diameter, respectively.

Due to the complexity of the co-axial, counterswirling air flows and the lack of adequate advanced diagnostics, few studies have been conducted on the two-phase behavior in the presence of such flows. Only recently have such flows been considered in a series of tests conducted at the UCI Combustion Laboratory (e.g., Wang et al., 1991a, b, c; 1992a).

The studies have been conducted at two scales. First, tests have been completed in a 3×-scale model. Secondly, measurements have been acquired in production hardware (i.e., "1×-scale"). While the purpose of the tests was to provide data in support of spray modeling, the results offer a unique opportunity as well to study (1) the extent to which the results scale on the basis of geometric similarity, and (2) the behavior of droplets at two geometrically similar scales.

In the present study, the time-averaged droplet size and velocity distributions are compared downstream of the production hardware and the 3×-scale model of the swirl cup. The liquid and air mass flow rates in the 1× test are about 1/9 of those in the 3× test, following the ratio of the air inlet area of the practical swirl cup to that of the 3×-scale model swirl cup. The purpose of this choice was to maintain a constant velocity from the swirling air outlet and a constant liquid loading rate (or air-to-liquid ratio) for both the 1×- and 3×-scale tests.

Experiment

Swirl Cup Assembly. Hago simplex atomizers, having flow numbers of 0.65 and 7.30 (based on ratio of flow rate, in lb/hr, to square root of injection pressure differential, in lb/in.²), were used in the 1×- and 3×-scale tests, respectively. A 6.35 mm polycarbonate honeycomb (101.6 mm thick) was placed 50 mm above the top of the swirl cup in both cases to provide a uniform velocity profile at the entrance plane to the swirlers.

Characterization Chamber. Two different characterization chambers were utilized. Although not specifically designed for these tests, each chamber was similar in design, and that used for the 3×-scale test was a 2.7-scale version of that used for the 1×-scale tests. In both chambers, the test article was centrally located within a square duct (495 mm × 495 mm for 1×-scale; 1330 mm × 1330 mm for 3×-scale) and oriented downward. The test article was attached to a vertical traverse, which was connected to the chamber. The chamber itself was suspended from an optical table using a two-dimensional traverse, thus giving the test article three degrees of freedom. In each case, the diagnostics were fixed, and the test article was moved. Additional details about each facility are available elsewhere (3×-scale: Wang et al., 1990; 1×-scale: Wang et al., 1991c, and McDonell and Samuelsen, 1991).

Instruments. A two-component phase-Doppler interferometer (PDI) (Aerometrics Model 3100-S) was used to measure the droplet size and velocities. An Ar⁺ laser provided the laser

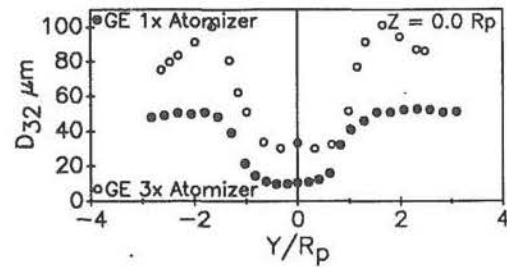


Fig. 2 Comparison of D_{32} between atomizers in the absence of the swirl cup assemblies

beams for the PDI measurements. The PDI setup used for both tests is shown in Table 1.

Test Condition and Sample Points

Test Condition. The inlet area of the swirlers for the production swirl cup is 1/9 of the 3×-scale model. To make the air outlet velocities through the 1× swirlers the same as those of the 3×-scale model, the 1×-scale tests were conducted at an air flow rate of 0.017 kg/s (30.2 scfm), which is 1/9 of the air flow rate used in the 3×-scale test.

Water was used in both tests. To maintain the liquid-to-air ratio the same as a stoichiometric ratio of a kerosene fuel (about 14.78), the liquid flow rate of the production and 3×-scale swirl cups should be 1.1 g/s and 10.0 g/s, respectively. While the 3×-scale tests were conducted at 10.0 g/s (Wang et al., 1991a, b), the 1×-scale hardware was operated at 0.86 g/s due to flow limitations in the test stand. This provided a liquid-to-air loading rate of 5.0 percent rather than 6.5 percent in the 3×-scale model test. However, the swirl cup flow field is dominated by the aerodynamics (Wang et al., 1991a, b), and this difference is considered negligible with respect to affecting both the gas-phase flow and droplet dispersion.

Sample Points. The measurements were conducted at three axial locations: $Z = 1.75, 2.75,$ and $3.75 R_p$ (where R_p is the radius of the primary venturi exit plane), and along the centerline of the swirl cup. The origin of the coordinates is at the center of the primary venturi exit plane. R_p for the 1×- and 3×-scale fixtures is 9.7 mm and 29.2 mm, respectively.

Results and Discussion

From the myriad of data collected, selected measurements are presented and specific characteristics are identified that are particularly germane to the behavior observed at both scales.

Atomizer Comparison in the Absence of the Swirl Cup. The two atomizers were characterized in the absence of the swirl cup assemblies to provide a baseline against which to compare differences observed in the presence of the swirl cup. An example is shown in Fig. 2. While large differences in D_{32} are observed due to the geometric difference in size and the order of magnitude difference in mass flow, far less difference is observed in the presence of the swirl cup assemblies.

Comparison of 1×- and 3×-Scale Swirl Cup Results. In the following, comparisons are presented for radial profiles at three axial planes ($Z = 1.75 R_p, 2.75 R_p,$ and $3.75 R_p$). In addition, for the velocity results, a centerline profile is included and appears in the top portion of the figure. Data are provided for the following representative droplet size groups:

- "Small" 11–20 μm
- "Medium-Sized" 30–40 μm
- "Large" 74–88 μm

Droplet Size and Data Rate. As shown in Fig. 3, the dif-

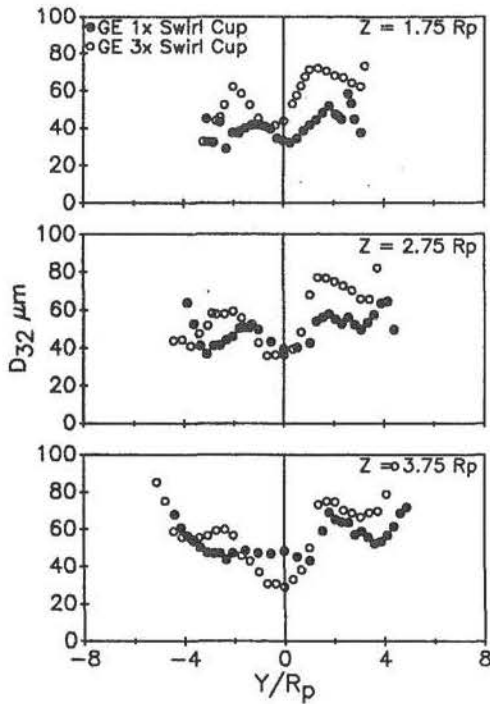


Fig. 3 Comparison of droplet distribution D_{32}

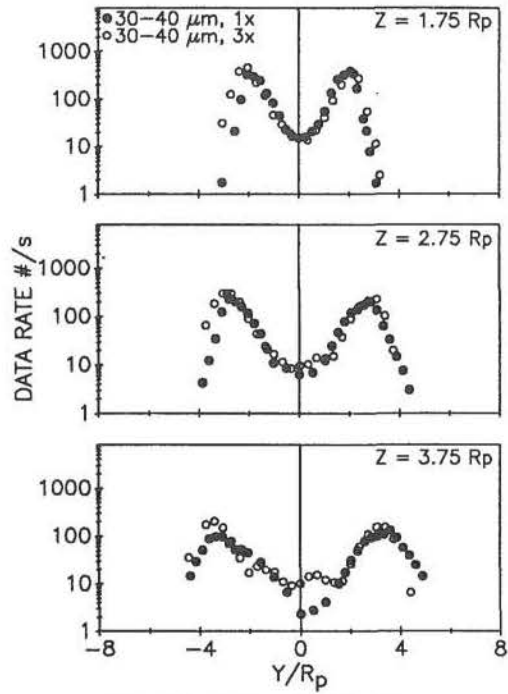


Fig. 4(b) Medium-sized droplets

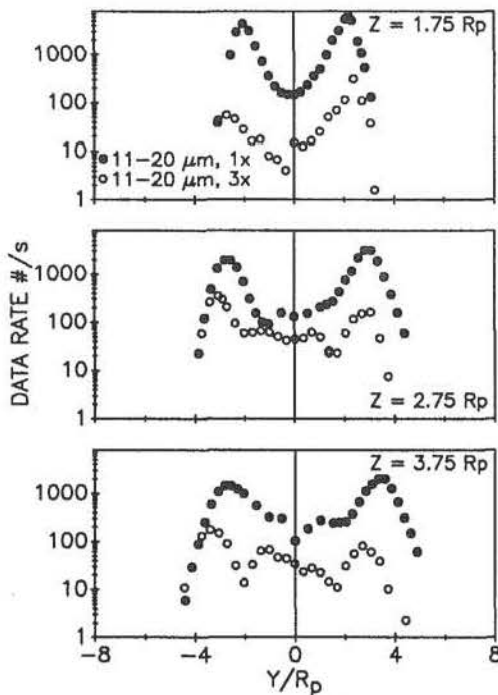


Fig. 4(a) Small droplets

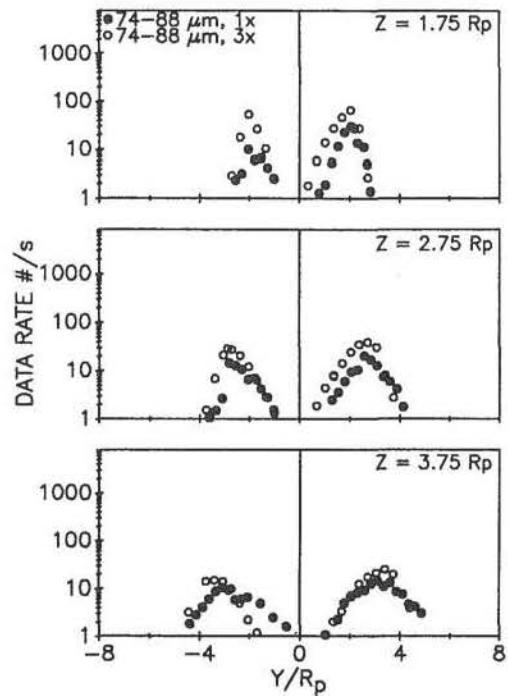


Fig. 4(c) Large droplets

Fig. 4 Comparison of droplet data rate

ferences in D_{32} are substantially reduced in the case of the swirl cup. While the D_{32} in the 3 × -scale case is systematically greater than in the 1 × case, the differences are reduced as the flow evolves downstream. The larger droplet size distribution for the 3 × -scale case is attributed to the differences in the initial droplet size distribution.

Additional insight is offered by the data rate results shown in Fig. 4. Compare, for example, the data rate of droplet arrival for the large and small droplets. At the first axial location ($Z = 1.75 R_p$), the data rate of the small droplets is greater

for the 1 × -scale (Fig. 4a), and the data rate for the larger droplets is greater for the 3 × -scale (Fig. 4c). Note the remarkable correspondence for the medium-sized droplets (Fig. 4b). This is the one large population of droplets that both scales share in common. This data set also reveals the first evidence of the effect of scale on droplet entrainment. At the centerline of the $Z = 3.75 R_p$ location, the data rate of the 1 × -scale falls relative to the 3 × -scale. These data, along with the mean axial and radial velocity data, reveal a disproport-

tionate entrainment of medium-sized droplets in the $3\times$ -scale case. Note also the associated impact on the D_{32} results at $Z = 3.75 R_p$ (Fig. 3). The twin-peak droplet data rate distributions in both cases suggest that the region downstream of the primary venturi is highly populated with droplets and thus high in liquid volume flux.

Mean Axial Velocities. Figure 5 presents results for the mean axial velocity. At the exit of the swirl cup, the axial velocity profiles of the continuous phase are identical for both cases (Fig. 5a). Downstream, modest but significant deviations occur. For example, the centerline profile reveals that a slightly longer recirculation zone exists downstream in the $3\times$ -scale test and the $Z = 3.75 R_p$ profile shows that the recirculation zone is wider as well. This is attributed to differences in entrainment rates between the two cases.

The $1\times$ -scale data at $Z = 3.75 R_p$ also reveal an asymmetry in the flow of the practical hardware. The flow field of the $3\times$ -scale model swirl cup is, in contrast, symmetric due to a stronger axial momentum.

The behavior of the droplets is shown in Figs. 5(b-d). The small droplets for both the $1\times$ - and $3\times$ -scale tests mirror the continuous phase (Fig. 5b) with one notable exception. At $Z = 1.75 R_p$, the small droplets in the $1\times$ -scale test have not fully relaxed to the continuous phase velocity. This is the first concrete example of the differences in time between the two scales for droplets to acclimate. The medium-sized droplets in the $3\times$ -scale test also reflect this (Fig. 5c). In addition,

the large droplets in the $3\times$ -scale case are recirculated at $Z = 3.75 R_p$, whereas those in the $1\times$ -scale case are not (Fig. 5d). The differences are attributed to the relatively long distance traveled from the atomizer to the same geometrically analogous points in the $3\times$ -scale test compared to the $1\times$ -scale test. Given that the droplet velocities are similar in each case, the medium-sized droplets have more time to approach the velocity of the continuous phase at the same geometrically analogous point in the $3\times$ -scale test than in the $1\times$ -scale test. Note the relatively analogous mean axial velocities at the first axial location for both cases.

Mean Radial Velocities. Figure 6(a) compares the mean radial velocities of the continuous phase. Positive values on the $+Y$ side and negative values on the $-Y$ side indicate velocities away from the centerline.

Near the swirl cup, the velocities scale remarkably well. Note in particular the evolution of the $3\times$ -scale mean radial velocities downstream. At $Z = 3.75 R_p$, for example, away from the centerline the flow is radially outward, whereas close to the centerline the flow is toward the centerline. Downstream of the $Z = 1.75 R_p$ location, the asymmetry in the production hardware is clearly evident. Both the centerline and radial profiles reveal a nonzero centerline velocity due to a mismatch of the aerodynamic and geometric centerlines.

As with the mean axial velocity, the radial velocities of the droplets are well scaled at the upstream location $Z = 1.75 R_p$. Downstream, the mean radial velocities for the small (Fig. 6b)

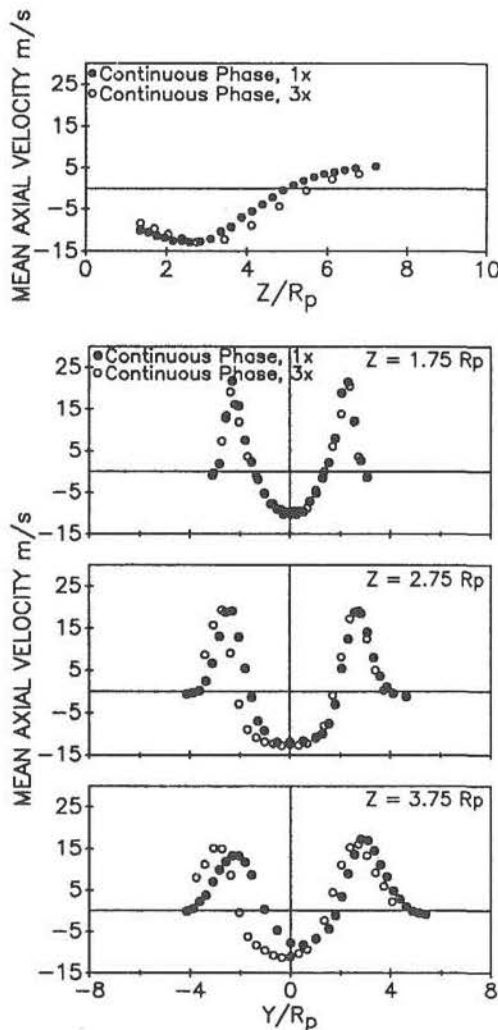


Fig. 5(a) Continuous phase

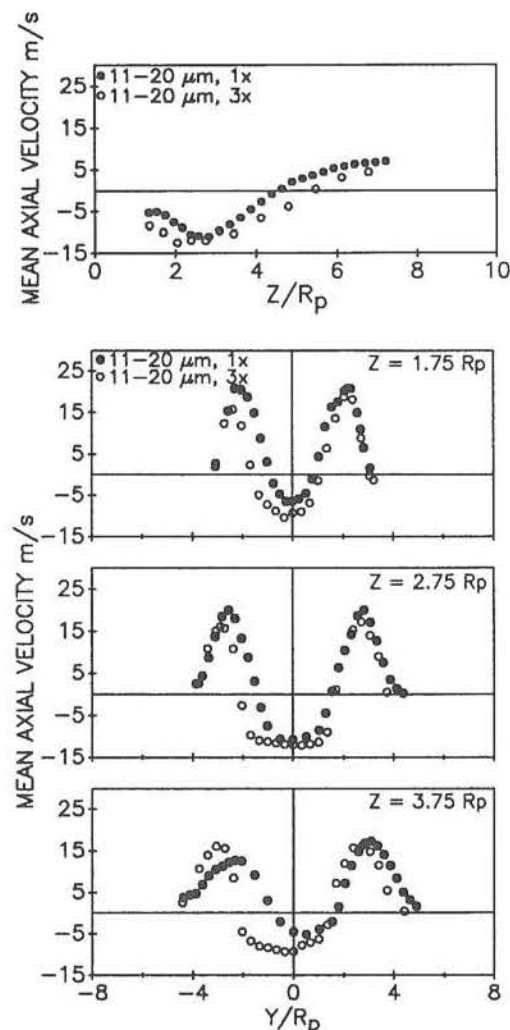


Fig. 5(b) Small droplets

Fig. 5 Comparison of mean axial velocity

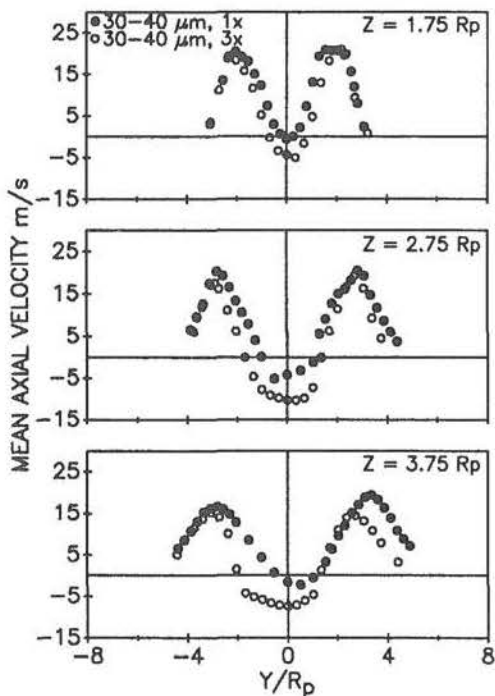
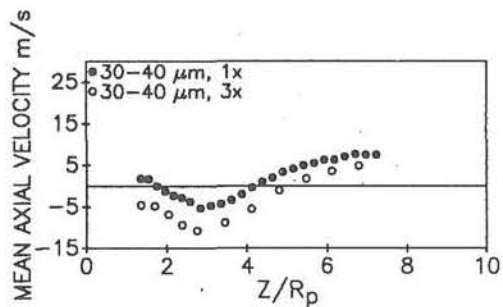


Fig. 5(c) Medium-sized droplets

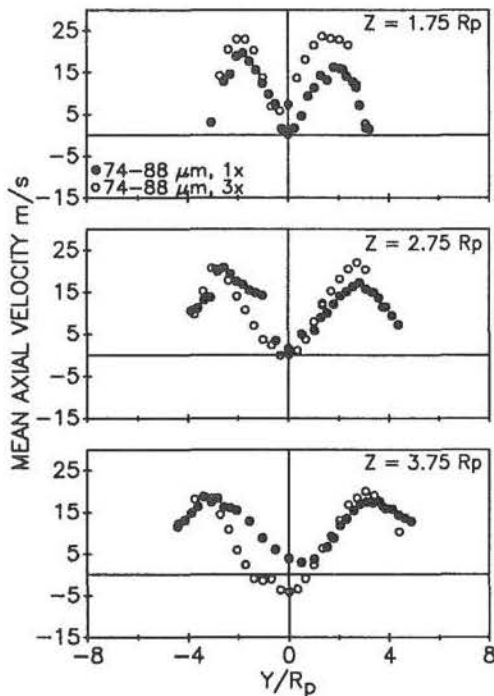
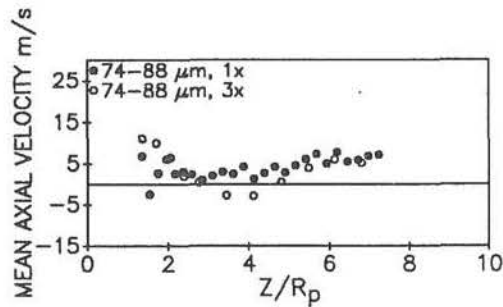


Fig. 5(d) Large droplets

Fig. 5 (continued)

and medium-sized (Fig. 6c) droplets reflect an asymmetry in the 1× test observed in the continuous phase. Because of the insensitivity of the large droplets to the influence of the gas-phase flow field, the mean radial velocity of the large droplets is more symmetric, in the 1× test, than that of the small and medium-sized droplets (Fig. 6d).

Noteworthy at $Z = 3.75 R_p$ is the inward flow of small- and medium-sized droplets to the centerline for the 3×-scale case. This again mirrors the continuous phase. The large droplets are unaffected.

Mean Tangential Velocities. The continuous phase mean tangential velocities are presented in Fig. 7(a). Looking downstream from the swirl cup, positive values on the +X side and negative values on the -X side reflect counterclockwise rotation. At $Z = 1.75 R_p$, the results appear "noisy." In fact, the data reflect a subtle behavior and, at $Z = 2.75 R_p$, the results are similar. Specifically, the radial location where the peak tangential velocities occur is the same and the decay of the profiles is similar. Unlike the mean axial and radial velocities, the tangential velocities of both scales are not precisely matched at $Z = 1.75 R_p$. The droplet behavior provides the explanation.

The droplet mean tangential velocities, presented in Figs. 7(b-d), provide especially interesting insights with respect to the effect of scale. In particular, the droplet mean tangential

velocity distributions display differences in magnitude and trend not observed in either the axial or radial velocity.

The mean tangential velocity distribution of the small droplets is presented in Fig. 7(b). The data for the small and medium-sized droplets in the 1×-scale test reveal a twin-peak distribution on either side of the centerline, with one inside the recirculation zone and the other outside of it. To understand the peaks, the sources from which droplets emanate to this point must be identified: (1) droplets recirculating while swirling counterclockwise, (2) droplets produced from the edge of the venturi (dominated by the counterclockwise-swirling secondary air), and (3) droplets injected directly from the atomizer, which are dominated by the clockwise rotating primary air. The relative contribution of these three sources results in strong bimodal velocity distributions (Wang et al., 1991b). What is different here is how the scale affects the sign of the peak. The major question is whether droplets directly injected from the atomizer with clockwise rotation can overcome the negative pressure gradient of the recirculation zone and penetrate to this point.

The small droplets (Fig. 7b) show two positive peaks at $Z = 1.75 R_p$. Outside the recirculation zone, the counterclockwise rotating secondary air is dominant, and inside the recirculation zone the counterclockwise rotating circulation overpowers the clockwise rotating droplets emanated from the atomizer directly. Note that the 3×-scale data are significantly

less precise than the mean axial and radial velocities at $Z = 1.75 R_p$. Clearly, scale and the associated differences in entrainment, and droplet residence time have a major impact.

The behavior of the medium-sized droplets is especially insightful. The $3\times$ -scale data at $Z = 1.75 R_p$ mirror the small droplet data. The $1\times$ -scale data, however, reveal a strong counterclockwise rotation in the recirculation zone, indicating that insufficient droplet residence time is available for these sized droplets to accelerate to the locally counterclockwise swirling flow.

Large droplets penetrate farther in the axial direction, as shown in Fig. 7(d). In this case, only two of the above sources contribute because very few large droplets are recirculated. As a result, the measurements consist of clockwise rotating droplets, which arrive directly from the atomizer and counterclockwise droplets arriving from the venturi. The behavior of the large droplets is similar for both cases because, compared to the small- and medium-sized droplets, their relaxation time is longer whereas their residence time is relatively shorter.

In both cases, with increasing axial distance downstream, the twin-peak distribution transitions into a single-peak distribution because the flow is dominated by the counterclockwise swirling secondary air flow.

Conclusions

The behavior of the continuous phase and droplets in the

flow field downstream of a production and a $3\times$ -scale model engine combustor swirl cup has been studied. Conclusions drawn from the study are as follows:

- The continuous phase scales well at the exit of the swirl cup in the present cases because the low liquid loading ratio has little effect on the flow. Farther downstream, scaling is difficult to evaluate because of differences in entrainment and the presence of asymmetries, especially with the production hardware.

- The droplets reflect the continuous-phase flow field to a varying degree depending upon droplet size or droplet relaxation time scale. The different behavior of droplets of different size can be explained successfully in terms of droplet relaxation time scale and the sources of droplets. The different behavior of droplets of same size in both cases can be interpreted by different droplet residence time reaching the same geometrically analogous point and the origins of these droplets.

- In spite of the differences in the atomizer characteristics, the behavior of the droplet size and velocity is similar in both the production ($1\times$ -scale) and $3\times$ -scale swirl cups, indicating that, for this particular hardware and operating condition, the continuous phase dominates the flow field and droplet dispersion.

- The droplet D_{32} in the $3\times$ -scale is generally greater than that in the $1\times$ -scale. This is due, in part, to differences in the initial droplet size distribution produced by the two atomizers.

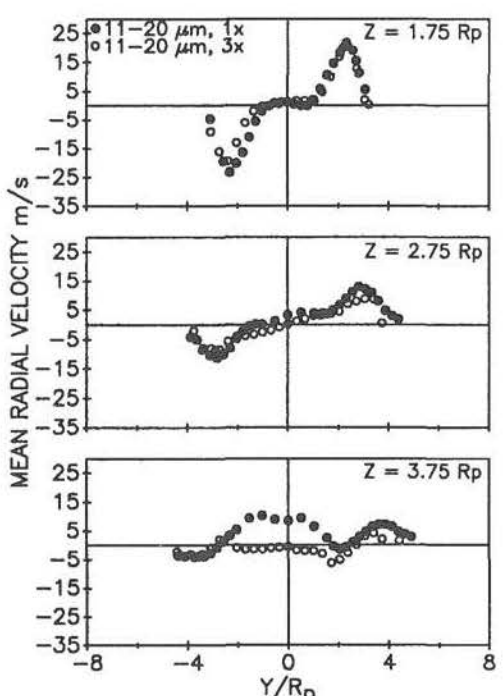
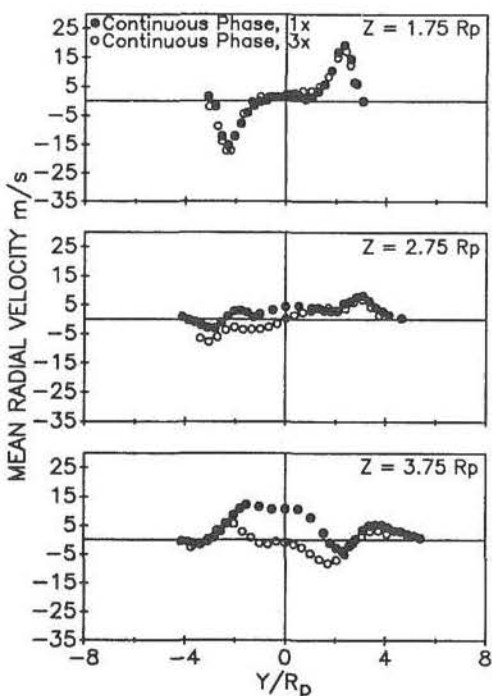
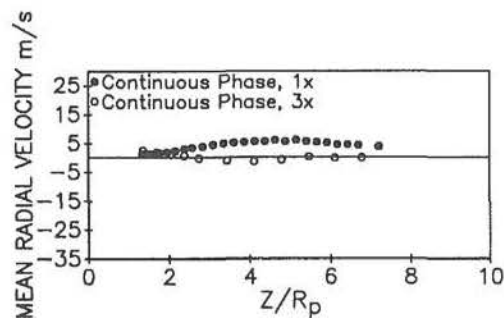
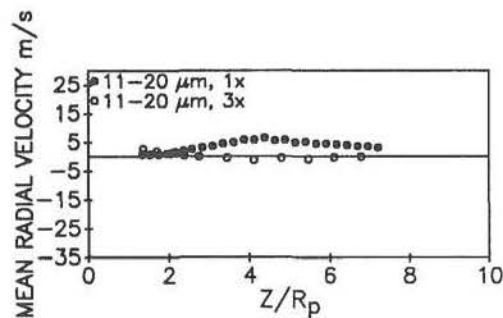


Fig. 6(a) Continuous phase

Fig. 6(b) Small droplets

Fig. 6 Comparison of mean radial velocity

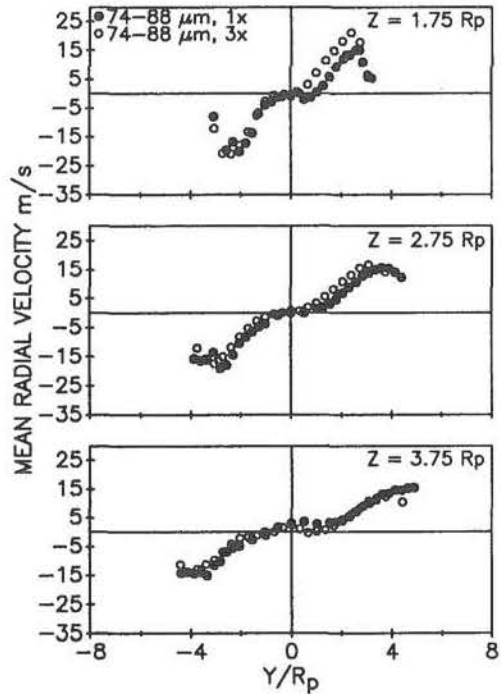
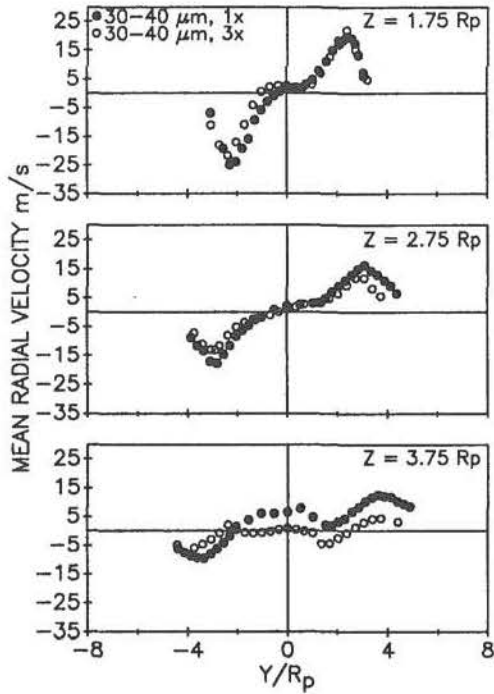
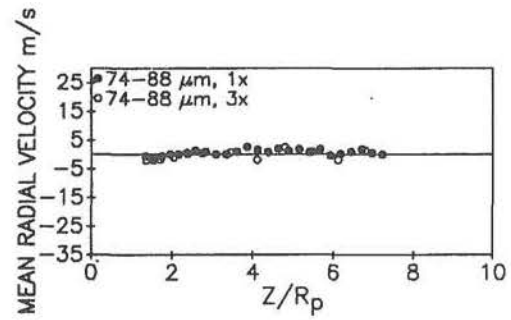
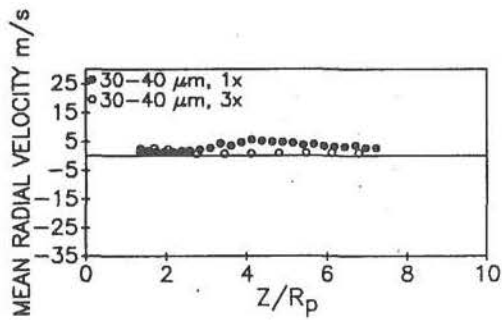


Fig. 6(c) Medium-sized droplets

Fig. 6(d) Large droplets

Fig. 6 (continued)

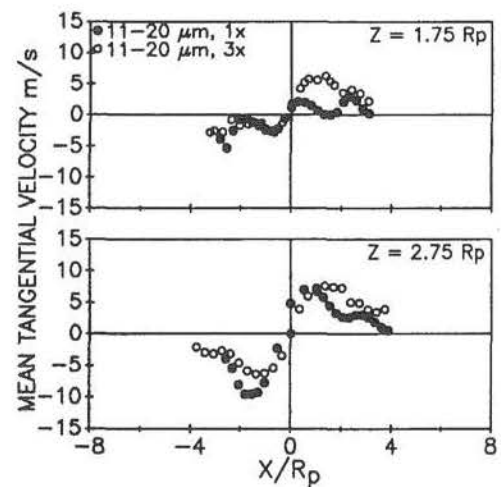
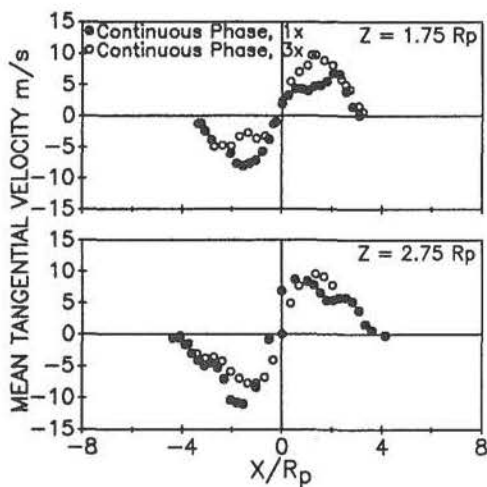


Fig. 7(a) Continuous phase

Fig. 7(b) Small droplets

Fig. 7 Comparison of mean tangential velocity

Nevertheless, the presence of the swirl cup tends to reduce these differences and provides more uniform and smaller droplet size distribution than using atomizer alone. The extent to which the aerodynamic flow and droplet formation from the

primary venturi contribute to differences observed cannot be determined at this point.

- The shear layer has a high droplet population and thus a high liquid volume flux for both 1x- and 3x-scale tests.

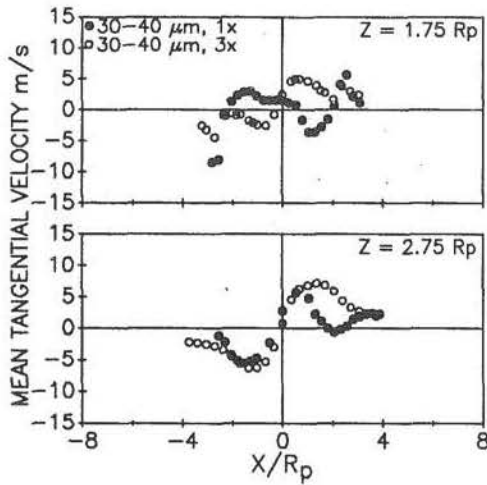


Fig. 7(c) Medium-sized droplets

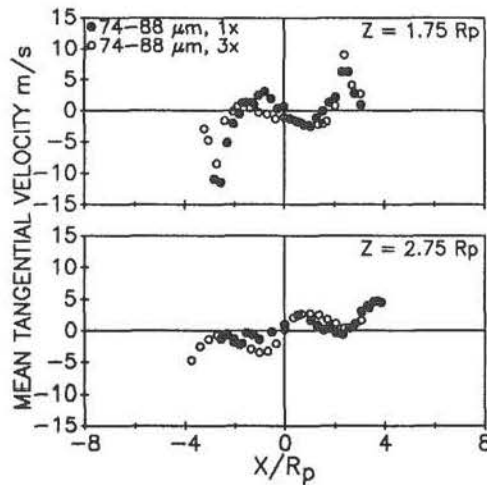


Fig. 7(d) Large droplets

Fig. 7 (continued)

Although the time-averaged information of the continuous phase and the droplets is essential to the understanding of the gas-phase flow field and droplet dispersion, the information

on the corresponding velocity rms and pdf is necessary for further insight into the gas-phase/droplet interaction, which will be discussed in the second part of this series study (Wang et al., 1992b).

Acknowledgments

The authors acknowledge financial support from GE Aircraft Engines, and the assistance of S. W. Lee with plotting part of the data and H. D. Crum with assembling the swirl cup hardware.

References

- Gouldin, F. C., Depsky, J. S., and Lee, S. L., 1983, "Velocity Field Characteristics of a Swirling Flow Combustor," AIAA Paper No. AIAA-83-0314.
- Habib, M. A., and Whitelaw, J. H., 1980, "Velocity Characteristics of Confined Coaxial Jets With and Without Swirl," *ASME Journal of Fluids Engineering*, Vol. 102, pp. 47-53.
- McDonell, V. G., and Samuelsen, G. S., 1991, "Gas and Drop Behavior in Reacting and Non-reacting Air-Blast Atomizer Sprays," *AIAA Journal of Propulsion and Power*, Vol. 7, pp. 684-691.
- Mehta, J. M., Shin, H. W., and Wisler, D. C., 1989, "Mean Velocity and Turbulent Flow Field Characteristics Inside an Advanced Combustor Swirl Cup," AIAA Paper No. AIAA-89-0215.
- Samimy, M., and Langenfeld, C. A., 1988, "Experimental Study of Isothermal Swirling Flow in a Dump Combustor," *AIAA Journal*, Vol. 26, No. 12, pp. 1442-1449.
- Vu, B. T., and Gouldin, F. C., 1982, "Flow Measurements in a Model Swirl Flow," *AIAA Journal*, Vol. 20, pp. 652-659.
- Wang, H. Y., McDonell, V. G., Sowa, W. A., and Samuelsen, G. S., 1990, "Swirl Cup Continuous and Discrete Phase Measurements in a 3x Scale Module," Final Report, UCI-ARTR-90-11, UCI Combustion Laboratory, University of California, Irvine.
- Wang, H. Y., Sowa, W. A., McDonell, V. G., and Samuelsen, G. S., 1991a, "Spray Gas-Phase Interaction Downstream of a Co-axial Counter-swirling Dome Swirl Cup," *Proceedings of the Fifth International Conference on Liquid Atomization and Spray Systems (ICLASS)*, pp. 687-694.
- Wang, H. Y., Sowa, W. A., McDonell, V. G., and Samuelsen, G. S., 1991b, "Dynamics of Discrete Phase in a Gas Turbine Co-axial, Counter-swirling, Combustor Dome Swirl Cup," AIAA Paper No. AIAA-91-2353.
- Wang, H. Y., McDonell, V. G., Sowa, W. A., and Samuelsen, G. S., 1991c, "Experimental Study of Single-Phase and Two-Phase Flow Fields Downstream of a Gas Turbine and a 3x Scale Model Combustor Swirl Cup," UCI-ARTR-91-6, UCI Combustion Laboratory, University of California, Irvine, CA.
- Wang, H. Y., McDonell, V. G., Sowa, W. A., and Samuelsen, G. S., 1992a, "Characterization of a Two-Phase Flow Field Downstream of a Gas Turbine Co-axial, Counter-swirling, Combustor Swirl Cup," AIAA Paper No. AIAA-92-0229.
- Wang, H. Y., McDonell, V. G., Sowa, W. A., and Samuelsen, G. S., 1992b, "Scaling the Two-Phase Flow Downstream of a Gas Turbine Combustor Swirl Cup: Part II—Fluctuating Quantities and Droplet Correlations," to be submitted to *ASME JOURNAL OF ENGINEERING FOR GAS TURBINES AND POWER*.